Khazar Journal of Science and Technology `Volume 9 №1 2025, 72-84
 DOI: 10.5782/2520-6133.2025.9.1.72

Fabrication and Tuning of the Morphological Characterization of Pvdf Based Electrospun Nanofibrous Material

Dilara Huseynova[1,2], Rasoul Moradi[2,3], Rasim Jabbarli[4]

[1] PhD student at Khazar University, Baku, Azerbaijan
[2] Nanotechnology Laboratory. Department of Chemical Engineering, School of Science and Engineering, Khazar University, Baku Azerbaijan
[3] Department of Chemical and Biological Engineering, College of Engineering, Korea University, Seoul, Korea
[4] Azerbaijan Institute of Physics Ministry of Science and Education of Azerbaijan.
Corresponding author: dilara.sadigova3377@gmail.com

Abstract

Surface protection has undergone a radical transformation thanks to nanocoatings, which provide novel approaches with enhanced durability, performance, and resistance. Because of their unique properties and wide range of applications, these coatings based on nanotechnology have attracted a lot of attention in recent years. In this work, the use of PVDF to produce electrospin fiber-oriented film coating material was examined. The technique employed to produce the aligned nanofibers is electrospinning. To investigate the alignment of the nanofiber material, we employed a directed electrical field in electrospinning apparatus. We employed atomic force microscopy (AFM) as our test. The impacts of the different types of collectors on the form of the fiber led to an increase in the alignment structure of nanofiber molecules. The results show that the morphological structure of the ordered organized nano-fibrous material that was generated is aligned.

Keywords: fibrous nanomaterial; PVDF; high electroactive phase; electrospinning; alignment; nanofiber; rotating drum.

Introduction

In the 1970s, PVDF, a polycrystalline polymer, began to attract scientific attention due to its remarkable piezoelectric qualities. A common piezoelectric semi-crystalline polymer, PVDF contains five distinct crystalline phases: α, β, δ, γ, and ε (Jayakumar *et al*., 2003). From the perspective of technical application, the α, β, and γ-phases are the most significant and prevalent among them. Due to its non-polar nature, the semi-helical alternative trans-gauche (TGTG') conformation of the α-phase, although being the most prevalent and thermodynamically advantageous

polymorph, is negligible in electronic applications. The β, γ, and δ-phases, on the other hand, are polar and hence electroactive because of the parallel alignment of their dipoles. The development of highly scalable polymer-based nanogenerators with high power density places a premium on the pseudohexagonal β-phase with all-trans (TTTT) conformation, which has exceptional piezo-, pyro-, and ferroelectric characteristics and strong spontaneous polarization. Improving the percentage of β counterpart is the primary issue when managing multi-phase PVDF for such applications. This can be accomplished in three main ways: (a) mechanically, by applying stress or tension through stretching, bending, twisting, or pressing (Prabhakaran and Hemalatha, 2013); (b) chemically, by adding appropriate filler materials (Huang, 2012) that can improve PVDF's mechanical, electrical, thermal, or optical properties through the right ion-dipole or dipole-dipole interactions. In addition to being economical, the third approach involves the creation of sophisticated multifunctional nanomaterials, which is significant from the standpoint of materials researchers (Bhattacharjee, *et al*., 2020; 4. Chen, *et al*., 2021). There is an obvious relationship between its crystal phases and its piezoelectric characteristics (Samadi, *et al.*, 2018). The most prevalent crystalline forms of PVDF are nonpolar α and polar β phases, with the β phase giving it its piezoelectric characteristics. In the past 10 years, enhancing the β phase while decreasing the α phase content in PVDF has been a prominent topic of attention. The β phase was increased by cold-drawing (stretching) (Martins, *et al*., 2014), high-pressure quenching (Tasaka and Miyata, 1985), and poling (applying a strong electric field) of PVDF (Ting, et al., 2013; Chowdhury, *et al*., 2021; Chowdhury, *et al*., 2020). By converting the α phase into the β phase under a strong electric field, electrospinning is an additional optional, straightforward, one-step technique for creating PVDF nanofibers. The β phase of the fibers is enhanced by the high voltage that is involved in this process (Mansouri, *et al*., 2019). Additionally, compared to solvent-cast films, electrospun fiber mats are far more mechanically robust and flexible (Ghosal, et al., 2018). Aligning PVDF mats enhances their mechanical, electrical, and electroactive properties, which boosts their efficacy and versatility in a variety of technological applications, especially in fields like energy harvesting, sensors, actuators, and coating materials. In the β phase of the PVDF molecule, alignment structure is observed.

An efficient method for continually and directly creating nanofibers is electrospinning. Nearly all polymer solutions, melts, emulsions, and suspensions with enough viscosity may be produced with polymer nanofibers using the electrospinning method, which is rather easy to use and convenient. Additionally, by incorporating trace quantities of polymers into the inorganic

precursors—which are typically thought of as nonspinnable—inorganic nanofibers may also be produced using electrospinning. By altering the spinning settings, the electrospun nanofibers' diameter may be adjusted from tens of nanometers to submicrons. The electrospun fiber-stacked nonwoven fabric has a porosity of about 80% and is a porous material with interconnecting submicron pores. The electrospinning fluid's unstable rheological characteristics, however, make it challenging to produce stable and continuous nanofibers with an average diameter of less than 100 nm. As a result, the electrospun nanofibrous membranes' separation applications are restricted to microfiltration, air filtration, or membrane substrate use. The development of electrospun nanofibrous composite (ENC) membranes was thus necessary to optimize the selectivity, permeability, and other separation capabilities of electrospun nanofibrous membranes in order to properly utilize them in other separation applications. The benefits of single-layered or single-component membranes are all present in composite membranes, but they offer greater versatility in terms of functional component selection (Meng, et al., 2023).

Handling an Electrospinning Procedure. The manufacturing factors, such as the applied voltage, the flow of liquid rate, and the distance between the spinneret tip and the collector, have a major impact on the synthesis of electrospun fibers and the controlling of their diameters. A high-voltage power source, a syringe pump, a spinneret (often a blunt-tipped hypodermic needle), and a conductive collector are the main parts. There are two types of power supplies: alternating current (AC) and direct current (DC). During electrospinning, surface tension leads the liquid to be extruded from the spinneret, creating a pendant droplet. The electric field is typically produced by applying a static DC high voltage to the spinneret (Xue, et al., 2019).

PVDF poling. The voltage's polarity, which can be either positive or negative, influences the kind of charges that build up on the jet's surface as well as the distribution of charged molecules inside the liquid. Certain materials, particularly electrolytes, have electrospinning capabilities that rely on the applied voltage's polarity (Terada, et al., 2012; Tong and Wang, 2012). In addition to the strength of the interactions between the jet and the external electric field, the applied voltage also directly affects the quantity of charges carried by the jet and the strength of electrostatic repulsion between the charges. Higher voltages often encourage the production of thinner fibers (Hu, et al., 2011), but they can also cause more fluid to be ejected, which results in fibers with larger diameters (Demir, et al., 2002). Electrospun fibers have also been electrospun using AC, however the jet behaves quite differently than in the DC case. Controlling the collecting mandrel's velocity in relation to the electrospinning suspension source has been used to address

fiber alignment (Ayres, et al., 2006; Nitti, et al., 2018; Mishra, et al., 2023; Sun, et al., 2010; Kim, et al., 2016; Martins, et al., 2014). Random fibers, one direction-oriented fibers, and circumferentially oriented fibers have all been produced using three different types of collectors: (1) static plate collector, (2) drum rotating collector, and (3) disk rotating collector (Ayres, et al., 2006). Electrospun chitosan nanofiber mats with random orientation could be produced using a static plate, but nanofiber mats that were aligned circumferentially and parallel to one another could be produced using a spinning disk and a rotating drum, respectively (Nitti, et al., 2018). For this investigation, the influence of this orientation has been examined and contrasted with fibers deposited utilizing various collector typologies. This technique involves aligning PVDF material using electrospinning equipment and employing atomic force microscopy (AFM) to analyze the structure and shape of the material.

The beta phase of polyvinylidene fluoride (PVDF) has unique properties that often make it desirable to enhance it. Numerous techniques have been devised to enhance the β-crystal concentration in PVDF (Mishra, *et al*., 2023). Converting α-crystal to β-crystal using solid-state drawing and/or strong electric field poling is an appealing method that can achieve a 50–85% increase in β-crystal content (Mishra, et al., 2023; Sun, et al., 2010; Kim, et al., 2016). Due to its strong ferroelectric, pyroelectric, and piezoelectric characteristics, the β-phase of PVDF is distinguished by the biggest spontaneous polarization and particular chain conformation per crystal unit cell. The highly electroactive β-phase in PVDF may be revealed by a number of techniques, including phase transition, solvent casting, nucleating fillers, electrospinning, and copolymerization of PVDF (Martins, et al., 2014; Harstad, et al., 2017; Ruan, et al., 2018; Ahn, et al., 2006; Lannutti, et al., 2007; Hunley and Long, 2008). With all of the dipolar moments oriented in the same direction, the β-phase is formed by electrospinning, which has emerged as a promising technique (Ahn, et al., 2006; Lannutti, et al., 2007; Hunley and Long, 2008). The nanofibers may be stretched mechanically to provide elongation forces during electrospinning and to arrange the lamellae into fibers that are aligned along the fiber axis (Zhou and Wu, 2015).

To improve alignment molecular structure, we queried PVDF in our experiment. Electric field stretching was employed for the aforementioned reasons in place of mechanical stretching force.

Materials and Methods. Polyvinylidene fluoride (PVDF) pellet has Mw = 1.8 × 104 with linear chemical structure $(-CH_2CF_2-)_n$ were purchased from Sigma-Aldrich,. Acetone and N, N-dimethylformamide (DMF) were purchased from Sigma-Aldrich Fe_3O_4 was obtained from Sigma-Aldrich

with an average particle size of 20-30 nm Polysorbate Tween purchased from Sigma-Aldrich and metal bar.

PVDF solution preparation. PVDF powders were dissolved using a magnetic stirrer in a 250 ml beaker at 35 rpm for two hours at a maximum temperature of 35°C. The mixture of organic solvents, DMF/acetone = 1/1 at 10 wt% (w/w), was stirred. Once the PVDF solution had completely dissolved, it was ultrasonically cleaned for two hours using the Ultrasonic Cleaner Digital Pro until it was homogeneous and bubble-free (figure 1). A solution of Fe_3O_4 nanoparticles with a 1wt% concentration was prepared by dissolving Fe_3O_4 nanoparticle powders in 50ml of DMF and adding 10ml of Polysorbate Tween as a surfactant at 30˚C while stirring at 35 rpm for two hours. After two hours, sonication was performed to get a non-homogenous solution. Following ultrasonication, a two-phase solution was created, with the electrospinning process using the upper phase.

Preparation of aligned PVDF Fiber Mats. In this investigation, mechanical stretching forces were employed in the form of electric field stretching. To achieve the aforementioned goals, a metal bar was electrospun into the PVDF nanofiber preparation process (figure 2). A metal bar was added to the grinding line of machinery. In this method, highly aligned PVDF-Fe_3O_4 nanofiber material is obtained and the β-phase content is increased as needed. Using a flow rate of 15 milliliters per hour, an output voltage of 16 kV, and a rotating drum speed of 556 rpm, PVDF-Fe_3O_4 nanofiber was created. 4 cm separated the metal bar from the revolving collector. In order to create the PVDF-Fe_3O_4 composite material, the rotating drum speed was increased while the electrical field stretching flow rate (Fe_3O_4) = 0.5 ml/hr was the only source of force. To feed the polymer and Fe_3O_4 solution, a dual channel programmable syringe pump was developed. Both the drum spinning collector and the static plate collector have been employed independently (figure 3).

Morphological structure analysis. Atomic force microscopy (AFM) and optical microscopy are used to analyze morphological aspects. AFM is a novel technology that uses a thin tip to scan a material in order to gain images and map the surface's contours, usually at the atomic level. Three-dimensional topography and plainly identifiable morphological structure are features of AFM pictures. It is well known that a surface's topography has a significant impact on a material's bulk characteristics (Assender, *et al*., 2002). After bonding, atoms or molecules work together to produce bulk qualities, which are mechanical characteristics.

The AFM pictures of PVDF-Fe_3O_4 coating surfaces at constant humidity (RH 50%) are displayed in Figure 4,5,6,7. AFM pictures make it clear that the PVDF-Fe_3O_4 surfaces from different collectors have different

morphologies. The surfaces were gathered on the static metal surface and have a rough form (figure 5). As shown in the AFM picture on the 37.5 nm * 37.5 μm lateral area for PVDF-Fe_3O_4 thin film, which is gathered on the revolving drum surface, we noticed that it was made up of microparticles connected by fiber-like connections (figure 5). The alignment structure of a revolving drum is greater than that of a PVDF-Fe_3O_4 sample obtained from a stationary plate. These topological variations may be caused by of stretching polymer molecules by rotation of the polymer species' sputter and collector processes with the surface.

Abbott-Firestone curves are shown in the surfaces' atomic force microscopy (AFM) pictures (see figure 4). The curve that displays the percentage of material provided in relation to the covered area is known as the bearing ratio curve. The vertical axis displays the recorded heights and depths of the surface, while the horizontal axis displays the bearing ratio as a percentage. The percentage of a surface that falls above or below a specific depth is shown by a bearing ratio study. The PVDF-Fe_3O_4 film collected on the revolving drum has a lower Core roughness value (Sk = 164 nm) than the static drum (Sk = 743 nm), as shown by Abbott-Firestone curves. Abbott-Firestone curves, three-dimensional AFM images, and the topography of the PVDF fibers' outer surfaces created at different kinds of collectors demonstrate that an alignment structure

has been seen in the specimens recovered from spinning drums (figure 4, 5). The AFM histograms for the height pictures are displayed in Figure 6. The surface texture is associated with the height distribution histograms. The statistical distribution of the z-values (heights) in a topographical picture is shown by the height histogram. The graph of columns that follow (or bins) is known as a histogram. Each column in the histogram represents a range of heights. The number of picture pixels with a height value within the specified range is shown by the height of each column. The red triangle has been positioned slightly below the surface level, and the blue triangle has been set to the lowest height value in order to calculate the volume of each pit. The height difference between the two peaks, calculated as the average pit depth, is around 0.4 nm. The void volume determined by the histogram for the samples from the static metal plate and revolving drum is 12352 μm^3 and 9194 μm^3, respectively. An imbalance in the height distribution graph was evident in the 3D picture as well as in the rough sample taken from the static drum. In addition to reaching the lowest roughness, the samples from the revolving drum also showed the required uniform height distribution.

The spatial characteristics that determine the surface periodicity and anisotropy include Srwi. The 2D Fourier transform of sample surface maps provides the basis for calculating the spatial parameter. The radial wave

index is known as the Srwi. It displays the size of the main radial wavelength and describes the sample surface's spatial structure. The 2D Fourier map's radial spectrum contained the dominating wavelength (Srw). The amplitude values related to M/(2–1) equally-spaced semi-circles, with the center at the center of the 2D Fourier map, are added up to determine the radial spectrum. The semicircles' radial is expressed in pixels, and r falls between 1 and 2, M/2–1. Compared to a static drum, the dominating wavelength has a higher value for the revolving drum sample. The ratio of the dominant wavelength's average amplitude to total amplitude is known as Srwi. Additionally, Srwi fluctuates between 0 and 1. This value is near zero if the dominating wavelength is present. This value is around 1 in the absence of a dominating wavelength (Tilinova, et al., 2024). Figure 7 shows the radial frequency distributions for PVDF -Fe_3O_4 fibers (10 wt,%) manufactured at two different types of collectors.

By employing several kinds of collectors, various fiber architectures were produced. Figure 8 summarizes the surface characteristics of the AFM image for pristine PVDF-Fe_3O_4 nanofibrous film material utilizing several kinds of drums. Nanofiber mats with random orientation may be produced using a static metal plate, while aligned nanofiber mats could be produced using a spinning drum. Additionally, a metal bar was fastened during the electrospinning process to create a stretching electric field. In this way, the morphology of the PVDF-Fe_3O_4 surfaces was enhanced.

Conclusions

In this study, we produced a pure PVDF-Fe_3O_4 fibrous film substance. From the AFM imaging results, it is evident that the aligned nanofibers were created using the electrospinning approach. To examine their form and structure, we produced highly aligned nanofibrous film material using a directed electric field in electrospinning equipment. We used AFM, or atomic force microscopy. By switching between two different kinds of collectors throughout the electrospinning process, the morphology of the electrospun PVDF-Fe_3O_4 fibers was examined. A static plate may be used to construct nanofiber mats with random orientation, whereas a rotating drum was used to create aligned nanofiber mats. The electrospinning process using a drum that rotates and the presence of an external molecular stretching field will be among the primary topics of the forthcoming studies on nanofibrous PVDF-Fe_3O_4 coated composite material.

Figure 1. 10 wt,% PVDF-Fe_3O_4 nanofibrous material preparation steps: a) PVDF solution preparation with hot plate, ultrasonic bath and plastic syringe, b) electrospinning equipment

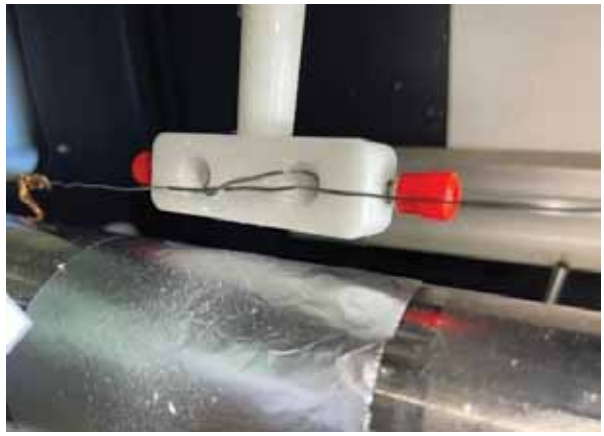

Figure 2. Joining metal bar to the electrospinning equipment

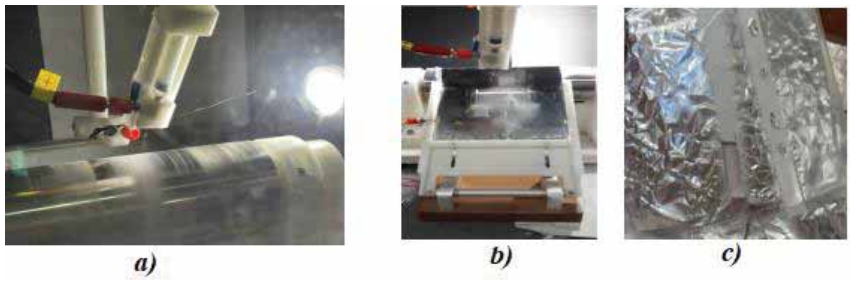

Figure 3. Using different types of collectors in electrospinning (Voltage - 16 kV): a) Rotating drum (Rotating Drum speed = 556 rpm; b) Static metal plate c) 10 wt, % PVDF-Fe_3O_4 nanofibrous sample on the surface of aluminum foil.

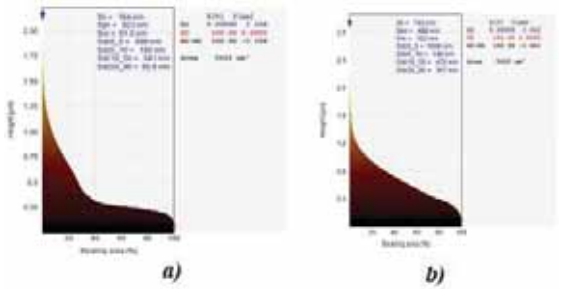

Figure 4. The Abbott-Firestone curve for PVDF-Fe_3O_4 (10 wt, %) fibers prepared at different types of collectors: (a) sample from rotating drum, (b) sample from static drum**.**

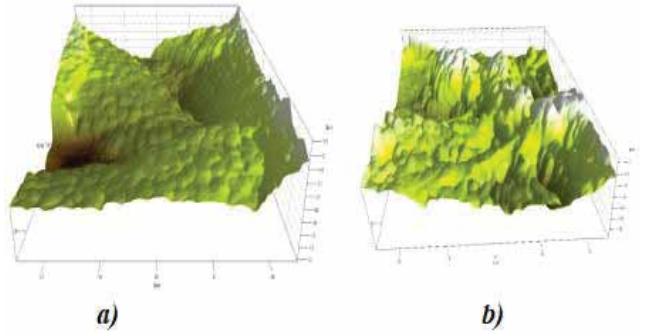

Figure 5. Three-dimensional AFM images of the outer surfaces of the PVDF-Fe_3O_4 fibers (10 wt, %) prepared at different type of collectors: (a) sample from rotating drum, (b) sample from static drum.

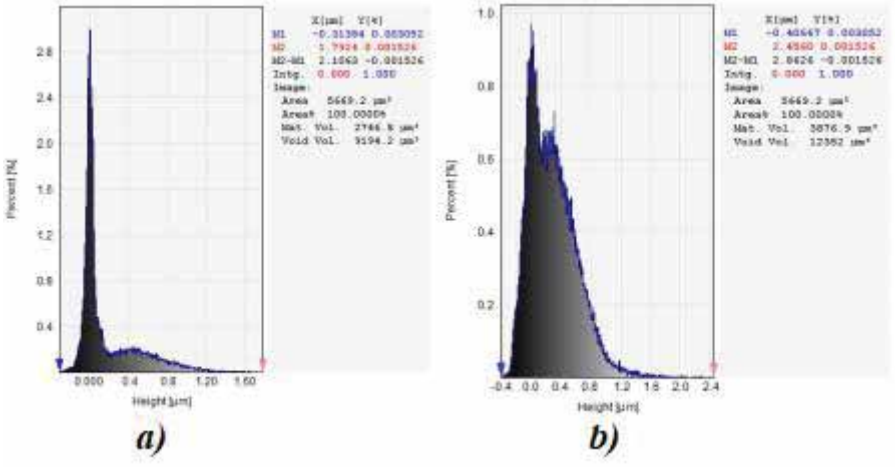

Figure 6. Surface roughness study histograms of the height distribution graphs of PVDF-Fe_3O_4 fibers (10 wt,%) made at various collector types: (a) a revolving drum sample; (b) a static drum sample. The image's minimal

height is shown by the blue cursor, while the bearing plane or surface level is indicated by the red cursor marker, which is positioned directly below the higher peak.

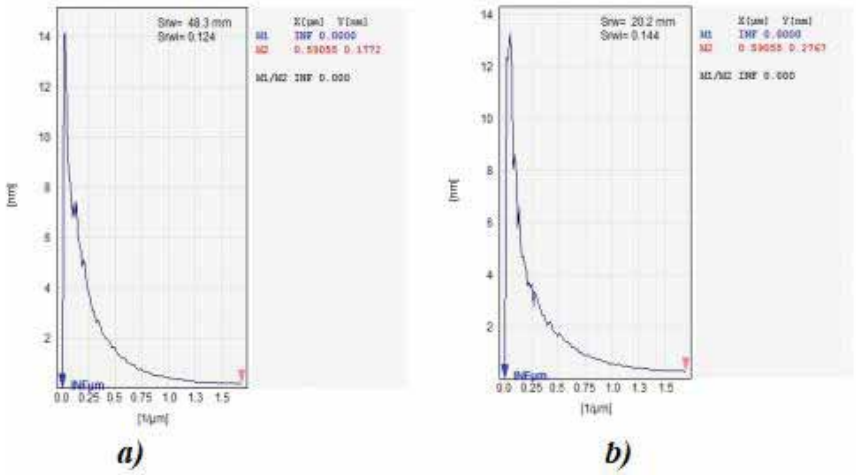

Figure 7. Radial Frequency profile for PVDF-Fe_3O_4 fibers (10 wt, %) prepared at different types of collectors: (a) sample from rotating drum, (b) sample from static drum

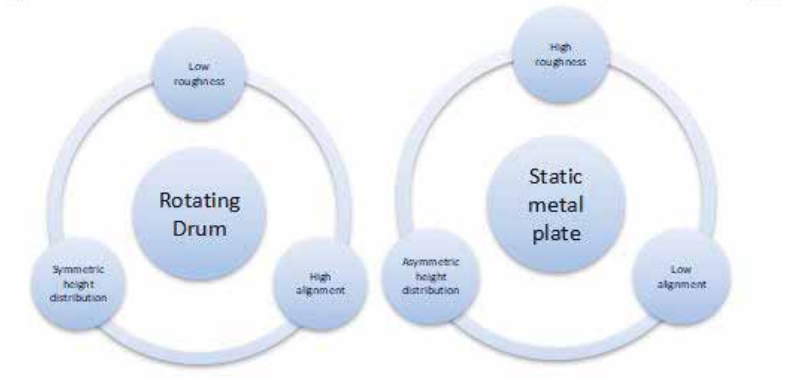

Figure 8. Summarization for AFM image surface parameters of PVDF-Fe_3O_4 fibers (10 wt, %) prepared at different types of collectors.

References

Jayakumar, O.D., Mandal, B.P., Majeed, J., Lawes, G., Naik, R., & Tyagi, J. M. (2013). Inorganic–organic multiferroic hybrid films of Fe3O4 and PVDF with significant magneto-dielectric coupling. 1, 3710–3715.

Prabhakaran, T., & Hemalatha, J. (2013). Ferroelectric and magnetic studies on unpoled poly (vinylidine fluoride)/Fe3O4 magnetoelectric nanocomposite structures. Mater. Chem. Phys. 37:781–787.

Huang, Z.Q., Zheng, F., Zhang, Z., Xu, H.T. & Zhou, K.M. (2012) Performance of the PVDF-Fe3O4 Ultrafiltration Membrane and the Effect of a Parallel Magnetic Field Used during the Membrane Formation. Desalination, 292, 64-72.

Chen, D., Li, J., Yuan, Y., Gao, C., Cui, Y., Li, S., Liu, X., Wang, H., Peng, C., Wu, Z. A. (2021). Review of the Polymer for Cryogenic Application: Methods, Mechanisms and Perspectives. Polymers 2021, 13, 320.

Bhattacharjee, S., Mondal, S., Banerjee, A., & Kumar, K. (2020). Chattopadhyay. Souvik Bhattacharjee, Suvankar Mondal, Anibrata Banerjee, and Kalyan Kumar Chattopadhyay, Mater. Res. Express 7. Mater. Res. Express 7, 044001.

Samadi, A., Hosseini, S.M., & Mohseni, M. (2018). Investigation of the electromagnetic microwaves absorption and piezoelectric properties of electrospun Fe3O4-GO/PVDF hybrid nanocomposites. Org. Electron. 59, 149–155.

Martins, P., Lopes, A.C. & Lanceros-Mendez, S. (2014). Electroactive Phases of Poly (Vinylidene Fluoride): Determination, Processing and Applications. Progress in Polymer Science, 39, 683-706.

Tasaka, S., & Miyata, S. (1985). Effects of crystal structure on piezoelectric and ferroelectric properties of copoly (vinylidenefluoride-tetrafluoroethylene). J Appl Phys 57:906–910.

Ting, Y., Gunawan, H., Sugondo, A., & Chiu., C.W. (2013). A New Approach of Polyvinylidene Fluoride (PVDF) Poling Method for Higher Electric Response. Ferroelectrics, 446, 28–38.

Chowdhury, T., D'Souza, N., & Dahotre, N. (2021). Low-Cost Reliable Corrosion Sensors Using ZnO-PVDF Nanocomposite Textiles. Sensors, 21, 4147.

Chowdhury, T., D'Souza, N., Ho, Y.H., Dahotre, N., & Mahbub, I. (2020). Embedded Corrosion Sensing with ZnO-PVDF Sensor Textiles. Sensors, 20, 3053.

Mansouri, S., Sheikholeslami, T.F., & Behzadmehr, A. (2019). Investigation on the electrospun PVDF/NP-ZnO nanofibers for application in environmental energy harvesting. J Mater Res Technol, 8: 1608–1615.

Ghosal, K., Chandra, A., Praveen, G., Snigdha, S., Roy, S., Agatemor, C., Thomas, S., & Provaznik, I. (2018). Electrospinning over Solvent Casting: Tuning of Mechanical Properties of Membranes. Sci. Rep. 2018, 8, 5058. Sci. Rep. 2018, 8, 5058.

Meng, Z., Zhu, L., Wang, X., & Zhu, M. (2023). Electrospun Nanofibrous Composite Membranes for Separations February, Accounts of Materials Research 4(2).

Xue, J., Wu, T., Dai, Y., & Xia, Y. (2019). Electrospinning and Electrospun Nanofibers: Methods, Materials, and Applications, Chem Rev. 24; 119(8): 5298–5415.

Terada, D., Kobayashi, H., Zhang, K., Tiwari, A., Yoshikawa, Ch., & Hanagata, N. (2012). Transient ChargeMasking Effect of Applied Voltage on Electrospinning of Pure Chitosan Nanofibers from Aqueous Solutions. Sci. Technol. Adv. Mater, 13, 015003.

Tong, H-W., & Wang, M. (2012). Negative Voltage Electrospinning and Positive Voltage Electrospinning of Tissue Engineering Scaffolds: A Comparative Study and Charge Retention on Scaffolds. Nano LIFE, 2, 1250004.

Hu, J., Wang, X., Ding, B., Lin, J., Yu, J., & Sun, G. (2011). One-Step Electro-Spinning/Netting Technique for Controllably Preparing Polyurethane Nano-Fiber/Net. Macromol. Rapid Commun, 32, 1729–1734.

Demir, M.M., Yilgor, I., Yilgor, E., & Erman, B. (2002). Electrospinning of Polyurethane Fibers. Polymer, 43, 3303–3309.

Ayres, C., Bowlin, G., & Henderson S. (2006). Modulation of anisotropy in electrospun tissue-engineering scaffolds: analysis of fiber alignment by the fast fourier transform, Biomaterials, 27 (32): 5524–5534.

Nitti, P., Gallo, N., Natta, L., Scalera, F., Palazzo, B., Sannino, A., & Gervaso, F. (2018). Influence of Nanofiber Orientation on Morphological and Mechanical Properties of Electrospun Chitosan Mats, Hindawi Journal of Healthcare Engineering, Article ID 3651480, 12 pages.

Mishra, S., Mohanty, Z., & Nayak, S.K. (2023). Study of nonisothermal crystallization kinetics of unstretched and uni-axially stretched electroactive PVDF composite films, Macromol. Chem. Phys. 224 - 2200326.

Sun, L.L., Li, B., Zhang, Z.G., & Zhong, W.H. (2010). Achieving very high fraction of β-crystal PVDF and PVDF/CNF composites and their effect on AC conductivity and microstructure through a stretching process, Eur. Polym. J. 46: 2112–2119.

Kim, J. F., Jung, J. T., Wang, H. H., Lee, S. Y., Moore, T., Sanguineti, A., Drioli, E., & Lee, Y.M. (2016). Microporous PVDF membranes via thermally induced phase separation (TIPS) and stretching methods. Journal of Membrane Science, 509, 94-104.

Martins, P., Lopes, A.C., & Lanceros-Mendez, S. (2014). Electroactive phases of poly (vinylidene fluoride): Determination, processing and applications. Polym. Sci. 39, 683.

Harstad, S., D'Souza, N., Soin, N., El-Gendy, A.A., Gupta, S., Pecharsky, V.K., Shah, T., Siores, E., & Hadimani, R.L. (2017). Enhancement of $\boldsymbol{\beta}$-phase in PVDF films embedded with ferromagnetic Gd5Si4 nanoparticles for piezoelectric energy harvesting AIP Adv. 7, 056411.

Ruan, L., Yao, X., Chang, Y., Zhou, L., Qin, G., & Zhang, X. (2018). Properties and Applications of the ? Phase Poly (vinylidene fluoride). Polymers 10, 1.

Ahn, Y.C., Park, S.K., Kim, G.T., Hwang, Y.J., Lee, C.G., Shin, H.S., & Lee, J.K. (2006). Development of high efficiency nanofilters made of nanofibers. Curr. Appl. Phys. 6, 1030 (2006)

Lannutti, J., Reneker, D., Ma, T., Tomasko, D., & Farson, D. (2007). Electrospinning for tissue engineering scaffolds. Mater. Sci. Eng. C 27, 504.

Hunley, M.T., & Long, T.E. (2008). Electrospinning functional nanoscale fibers: a perspective for the future. Polym. Int. 57, 385.

Zhou, Z., & Wu, X.F. (2015). Electrospinning superhydrophobic–superoleophilic fibrous PVDF membranes for high-efficiency water–oil separation Mater. Lett. 160, 423–42794

Assender, H., Bliznyuk, V., & Porfyrakis, K. (2002). How Surface Topography Relates to Materials' Properties, Science, 297(5583): 973-976.

Tilinova, O.M., Inozemtsev, V., Sherstyukova, E., Kandrashina, S., Pisarev, M., Grechko, A., Vorobjeva, N., Sergunova, V., & Dokukin, M.E. (2024). Cell Surface Parameters for Accessing Neutrophil Activation Level with Atomic Force Microscopy. Cells, 13, 306.